Physica A 163 (1990) 410–428
North-Holland

BENDING ELASTICITY AND THERMAL EXCITATIONS OF LIPID BILAYER VESICLES: MODULATION BY SOLUTES

H.P. DUWE and E. SACKMANN
Physics Department, Biophysics Group, Technische Universität München, D-8046 Garching, Fed. Rep. Germany

We present high-precision measurements of the bending elastic moduli of bilayers of a variety of different lipids and of modifications of the flexural rigidity by solutes. The measurements are based on the Fourier analysis of thermally excited membrane undulations (vesicle shape fluctuations) using a recently developed dynamic image processing method. Measurements of the bending modulus as a function of the undulation wave vector provide information on the limitation of the excitations by the constraint of finite membrane area (surface tension effects) and by transient lateral tensions arising in each monolayer by restricted diffusion at high wave vectors. Measurements of the autocorrelation function of the undulation amplitudes provide a further test of the theoretical models. Studies of the effect of solutes show that cholesterol increases the bending modulus of dimyristoylphosphatidylcholine from $K_c = 1.\ 1 \times 10^{-12}$ erg to 4.2×10^{-12} erg (at 30 mol%). Incorporation of a short bipolar lipid reduces K_c to the order of kT. Finally we present a variety of shape changes of vesicle and provide evidence for the stabilization of metastable non-equilibrium shapes by lateral phase separation.

1. Introduction

Lipid bilayer vesicles fascinate physicists because of their peculiar elastic and dynamic properties which are dominated by a very soft bending elastic modulus of the order of $10\,kT$. They appeal to biophysicists since (despite of their simple structure) they exhibit typical mechanical and rheological features of cell membranes. The bending elastic modulus may be lowered by solutes towards the thermal energy in order to approach the limit of random surfaces. New fascinating phenomena arise in mixed bilayers where the coupling of lateral phase separation and curvature effects leads to a manifold of metastable vesicle shapes. By using dynamic image processing methods it has become possible to determine the mean square amplitudes and the correlation times of the thermal membrane excitations as a function of the wave vector in the optical regime which allows high-precision measurements of the bending elastic modulus. In the first part of the present contribution we summarize our recent measurements of the bending elastic moduli of bilayers of synthetic and natural

0378-4371/90/$03.50

lipids. In the second part we present a variety of vesicle shape changes which are governed by the membrane bending elastic properties.

2. Theoretical background of the method

It is generally accepted now that the thermal undulations of vesicles and also biconcave (and moderately swollen) erythrocytes can be described in terms of the quasi-spherical model first worked out by Helfrich [10] and Schneider [21] and subsequently improved by Peterson [17] and Millner and Safran [15] to include spontaneous curvature effects and to account for the suppression of long-wavelength modes (Duwe et al. [4]) by the constraint of constant area. The thermal excitations of quasi-spherical vesicles are described in terms of a spherical harmonics expansion ($Y_{lm}(\vartheta, \varphi)$) of the middle surface separating the two monolayers. The latter is determined by the radius $r(\vartheta, \varphi)$ (ϑ: polar angle, φ: azimuthal angle) which is

$$r(\vartheta, \varphi, t) = r_0\Big(1 + \sum_{l,m}^{\infty} a_{l,m}(t) Y_{l,m}(\vartheta, \varphi)\Big) , \tag{1}$$

where r_0 is the so-called equivalent radius. It is equal to the radius of a sphere of the same volume, V, as the vesicle.

For symmetric bilayers where spontaneous curvature effects can be ignored, the undulations are determined by the elastic energy (sign as in [15]):

$$E_c = \int_A (\tfrac{1}{2} K_c H^2 - \gamma)\, dA , \tag{2}$$

where H is the mean curvature: $H = 1/r_1 + 1/r_2$ (r_1, r_2 principal radii of curvature). γ is a Lagrange multiplier which accounts for the constraint of constant area. Physically it corresponds to the lateral tension which arises out of those excitational modes which require a larger excess area than available. Provided the excitation of the spherical harmonic models follows the equipartition theorem, the normalized mean square amplitudes of the spherical harmonic node characterized by the angular momentum (l) and magnetic quantum number (m) are giving by

$$\langle |a_{l,m}|^2 \rangle = \frac{k_B T}{K_c (l+2)(l-1)[l(l+1) - \tilde{\gamma}]} , \tag{3}$$

where $\tilde{\gamma} = \gamma r_0^2 / K_c$. As pointed out first by Brochard and Lennon [3], the damping of the membrane bending undulations is determined by the hydro-

dynamic flow of the enclosed and surrounding fluid and for that reason the modes are completely overdamped. The (temporal) autocorrelation function of the amplitudes $a_{lm}(t)$ are exponentials (Millner and Safran [15], Schneider et al. [21]):

$$\langle a_{l,m}(t)a_{l,m}(0)\rangle = \langle |a_{l,m}|^2\rangle \exp(-\omega_{l,m}t)\,, \tag{4}$$

where

$$\omega_{l,m} = \frac{K_c}{\eta r_0^3}\,(l(l+1)-\tilde{\gamma})/Z_l\,, \tag{5}$$

$$Z_l = \frac{(2l+1)(2l^2+2l-1)}{l(l+1)(l+2)(l-1)}\,. \tag{6}$$

It is important to note that equipartition is only possible if the flow within the bilayer is fast enough to accomodate for local density fluctuations (in each monolayer) associated with the undulations. A breakdown of the equipartition is indeed observed for membranes containing cholesterol (cf. section 4.).

Experimentally, the excitations of the vesicle have to be analysed in terms of the fluctuations of the contour observed in the phases contrast microscope. This is possible provided

1) the vesicle is quasi-spherical so that the image plane goes through its center of mass;
2) the time over which the fluctuations are observed is large compared to the response (=relaxation) time of the excitations.

Let the Fourier transform of the momentary contour at time t be

$$v(\varphi, t) = r_0 \sum_{q=0}^{q=q_{max}} \vartheta_q(t) \exp(-iq\varphi)\,, \tag{7}$$

where φ is the longitudinal angle. $v(t, \varphi)$ is determined by the deviation of the vesicle surface from the sphere at $\vartheta = \pi/2$ and by using eq. (1) one obtains for the Fourier component $v_q(t)$ of eq. (7).

$$v_q(t) = \frac{1}{2\pi} \sum_{l=q,m}^{l_{max}} a_{l,m}(t) \int Y_{l,m}(\pi/2, \varphi)\, e^{iq\varphi}\, d\varphi\,. \tag{8}$$

The sum starts at $l = q$ but the minimum of l must be larger than two. The mean square amplitudes of the contour fluctuations are then

$$\langle |v_q(t)|^2\rangle = \sum_{l=q,m}^{l_{max}} \langle |a_{l,m}(t)|^2\rangle P_{l,m}^2(\cos \pi/2)\,, \tag{9}$$

where $P_{l,q}(\cos(\pi/2))$ are the values of the Legendre polynomials in the equatorial plane. Thus the mean square amplitudes of the fluctuation of the contour are directly related to the mean square amplitudes of the spherical harmonics given in eq. (3). The sum in eq. (9) converges rapidly with increasing l and has been calculated for the quantum numbers $2 \leq q \leq 10$ up to $l = l_{\max} = 34$ [2, 5].

3. Experimental procedure

3.1. Preparation of thin-walled vesicles

Giant vesicles with diameters larger than 10 μm were prepared by the following procedure. The lipid or lipid mixture was dissolved in 2:1 chloroform/methanol (1 mM solution). 20 μl of this solution (containing about 2×10^{-8} mol or 10^{-5} g of lipid) was distributed as a thin film on the surface of a microscope cover glass. The solvent was evaporated by placing the substrate in a vacuum chamber for a minimum of one hour. The cover glass was inserted in a sample cell (where it served as the bottom window) and was fixed with silicon grease. The sample cell was filled with distilled water and the top closed (and sealed) with a second cover glass (the top window). The whole sample cell was inserted into a thermostated measuring chamber made of V2A steel. The temperature could be varied between 0 and 50°C by using Peltier elements which were cooled by water. The temperature in the sample chamber was measured with a Pt100 temperature sensor.

3.2. Experimental procedure used for Fourier analysis of vesicle contour fluctuations

The vesicles were observed and evaluated with an inverted Zeiss Axiomat microscope. It was mounted (on air cushions) on a heavy ground plate which was suspended at the laboratory ceiling to reduce vibrations caused by walking. A schematic view of the opticla set-up is shown in fig. 1. One advantage of the Axiomat is that the position of the image plane of the (infinity adapted) objective can be choosen at will. In this way a normal bright field objective can be used for phase contrast microscopy by placing a phase plate in the image plane which is far away from the ojective. For the present work a bright field air objective of magnification 50 × (Zeiss) was used. Since the working distance of the objective was only 300 μm, the vesicles near the bottom window of the sample cell had to be observed by an inverted microscope. Images of the vesicles selected were taken with a charge coupled device (CCD) camera (frame transfer camera, HR600M, Aqua-TV company, Kempten, FRG) onto

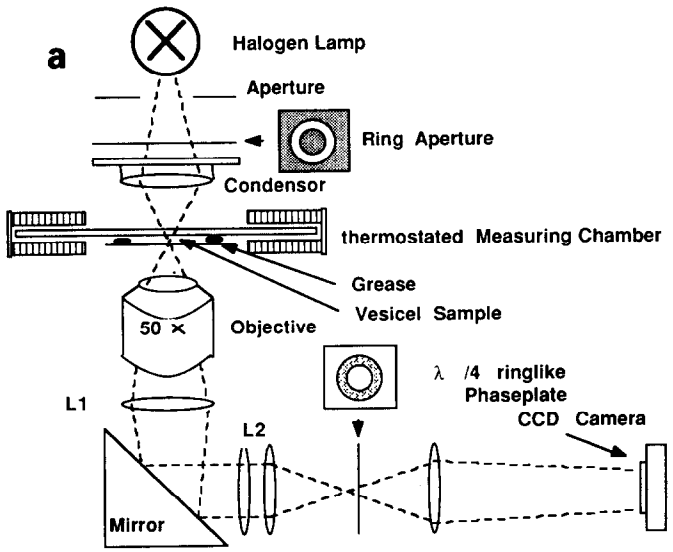

Fig. 1. (a) Schematic view of set-up used for observation of vesicle which is built around an inverted Zeiss Axiomat microscope. Since the focus of the objective is set at infinity its image plane can be positioned at will by using the lenses L_1 and L_2 and the mirror. Therefore a normal bright field objective (here: Zeiss 50×, Air, Pol, numerical aperature 0.95, working distance 300 μm) can be used for phase contrast microscopy by placing a (ring-like) phase plate in the image plane. The sample could be illuminated with a 100 W halogen lamp (Zeiss) or a high-pressure mercury lamp (HBO-100) with ultraviolett cut-off filter which improved the optical resolution. (b) DMPC-vesicle with intensity distribution (white shaky curve) along a direction indicated by the white straight line. The position of the contour is determined by the two minima in the intensity distribution.

which a section of $40 \times 40\ \mu m^2$ of the image plane was projected. The camera is connected to an image processing system (MAXVIDEO, DataCube Boston, USA) with VME bus and 059 operating system. With this system the images from the video camera are digitized 512×512 pixels and 256 gray levels.

A fast algorithm was developed which allowed to evaluate the (time-dependent) contour of a vesicle at a rate of 5–10 per second and to store the data in the computer memory. The procedure is illustrated in fig. 2. Since the phase shift of the light is maximal if it passes tangential to the vesicle surface, the transient contour (that is the equator of quasi-spherical vesicle) corresponds to a sharp minimum of the brightness of the image. First a starting point (coordinate x_0, y_0) of the contour is selected by the cursor. Each pixel has 8 neighbours which define 8 directions (numbered 0 to 7 in fig. 2). As second step the adjacent contour point is searched as follows: the intensity over three bands comprising 46 pixels and lying in three different directions of the eight are added-up. The position of the contour (x_1, y_1) adjoining the starting point (x_0, y_0) lies in the direction of minimum total intensity and is given by ($x_0 + 1$, $y_0 + 1$). The three test directions are determined by the direction of the previous step. The above procedure is repeated until one returns to the position of the starting point. The number of 46 pixels is of course arbitrary. It has been found optimal to account for the fact that the width of the intensity valley is 5 to 6 pixels (cf. fig. 2). After having determined (and stored) the positions of the contour the center of mass of the vesicle is determined according to

$$S_x = \frac{1}{K} \sum_{i=1}^{K} x_i, \qquad S_y = \frac{1}{K} \sum_{i=1}^{N} y_i\,, \tag{10}$$

where K is the number of pixels of the contour and is typically $K = 500$–1000. Now, the polar coordinates (φ_i, R_i) of the contour are determined with the center of mass as origin.

The Fourier decomposition of the contour is performed using a Fast Fourier Transform procedure [16]. For this procedure the contour line must be divided into 2^N equidistant points. Since the contour line is determined by 500–1000 pixels a new set of $2^9 = 512$ points ($R_{0,511}$) is determined from the original set ($R_{i,K}$) by averaging over the values lying within segments of opening angle $2\pi/128$.

The Fourier transformation yields complex Fourier coefficients,

$$c_q = a_q + \mathrm{i} b_q\,,$$

where q runs from -255 to $+255$. Of these the values for $0 \leq q \leq 10$ are stored.

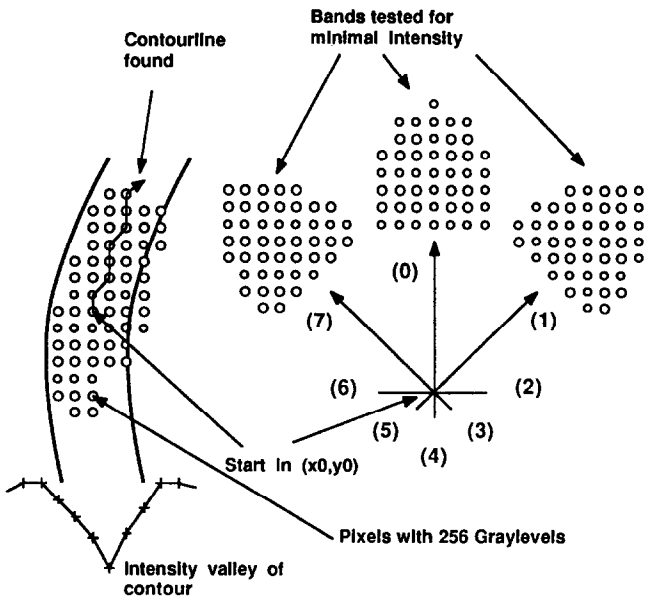

Fig. 2. Schematic representation of algorithm used to determine the transient contour of the vesicles. The starting point at (x_0, y_0) is selected interactively for the first time. Then the intensity over three bands comprising 46 pixels and lying in three different directions (of the eight possible) are added up to find the direction of minimum intensity. An example of the depth of the intensity valley is shown at the left lower corner. Note that the area covered by the bands of 46 pixels corresponds to about one point in the band.

As the next step, the mean square amplitude is determined as follows:

Since the excitation modes are statistically independent, the time average of the contour is determined by averaging over the Fourier coefficients of an arbitrary number of M-contours,

$$\bar{c}_{n,q} = \frac{1}{M} \sum_{n-M/2}^{n+M/2} (a_{i,q} + b_{i,q}) = \bar{a}_{n,q} + \bar{b}_{n,q} , \tag{11}$$

where n is an eligible number of that contour from which the procedure is started. It must be: $n \geqslant M/2$. The mean square amplitudes of mode q are finally given by

$$\langle |v_q(t)|^2 \rangle = \frac{1}{N} \sum_{1}^{N} \{(a_{i,q} - \bar{a}_{n,q})^2 + (b_{i,q} - \bar{b}_{n,q})^2\} . \tag{12}$$

The bending modulus is directly obtained from eq. (9). The average vesicle

radius is given by

$$r_0 = \sqrt{\overline{a_{n,0}^2} + \overline{b_{n,0}^2}}\,, \tag{13}$$

where $\bar{a}_{n,0}$, $\bar{b}_{n,0}$ are the averaged Fourier coefficients for $q = 0$.

4. Bending moduli of synthetic and natural lipids and the effect of cholesterol

Fig. 3(a) shows values of the bending modulus of DMPC bilayers as a funtion of the wave vector q characterizing the undulations of the contour (cf. eq. (7)) measured at 30°C. The K_c-value of the lowest order mode ($q = 2$) is clearly larger than that of the higher nodes ($q = 3$ to 10). The latter agree within experimental error although a shallow minimum appears to exist around $q = 5$. The average value of K_c obtained for $3 \leq q \leq 10$ is $K_c = (1.15 \pm 0.15) \times 10^{-12}$ erg. As demonstrated in fig. 3(b) it is essential to analyse a sufficiently large number of images in order to probe all excitational states of the vesicle. The average value of K_c decreases with the number of contours analysed that is the true bending elastic modulus is given by the asymptotic value of K_c. Fig. 4 shows measurements of the bending modulus, K_c, as a function of the wave vector q for DMPC containing 20 mol% and 30 mol% of cholesterol. A qualitatively different q-dependence as in fig. 3 is observed. As in the case of pure DMPC, the K_c-value for the lowest order mode ($q = 2$) is larger than for $q = 3$. However, at $q > 3$, K_c increases again with the wave vector. Below, this behaviour will be interpreted in terms of a reduction of the high order modes by the reduced flow of the bilayer.

Fig. 5 shows a summary of the average bending moduli of vesicles of DMPC. Altogether 26 vesicles were analysed. The ordinate of the histogram gives the number of cells yielding the same K_c-value. Clearly, four groups with averages of $K_c = 1.1 \times 10^{-12}$; $K_c = 2.1 \times 10^{-12}$; $K_c = 3.1 \times 10^{-12}$ and $K_c = 4.1 \times 10^{-12}$ erg are distinguished. The larger K_c-values are multiples of the miniumum value. This leads to the conclusion that these groups correspond to vesicles with shells composed of one, two, three and four bilayers.

Fig. 7 summarizes the values of the bending moduli of lipid bilayers determined in our laboratory. The two more exotic lipids 1, 2 di ($5C_1$ – 16: 0)-PC and galactosyldiglyceride are included in this figure. For comparison the value of K_c of erythrocytes measured by direct Fourier analysis of the membrane excitations by reflection interference contrast microscopy is also given. Each point corresponds to the measurement of one vesicle. The most remarkable results are:

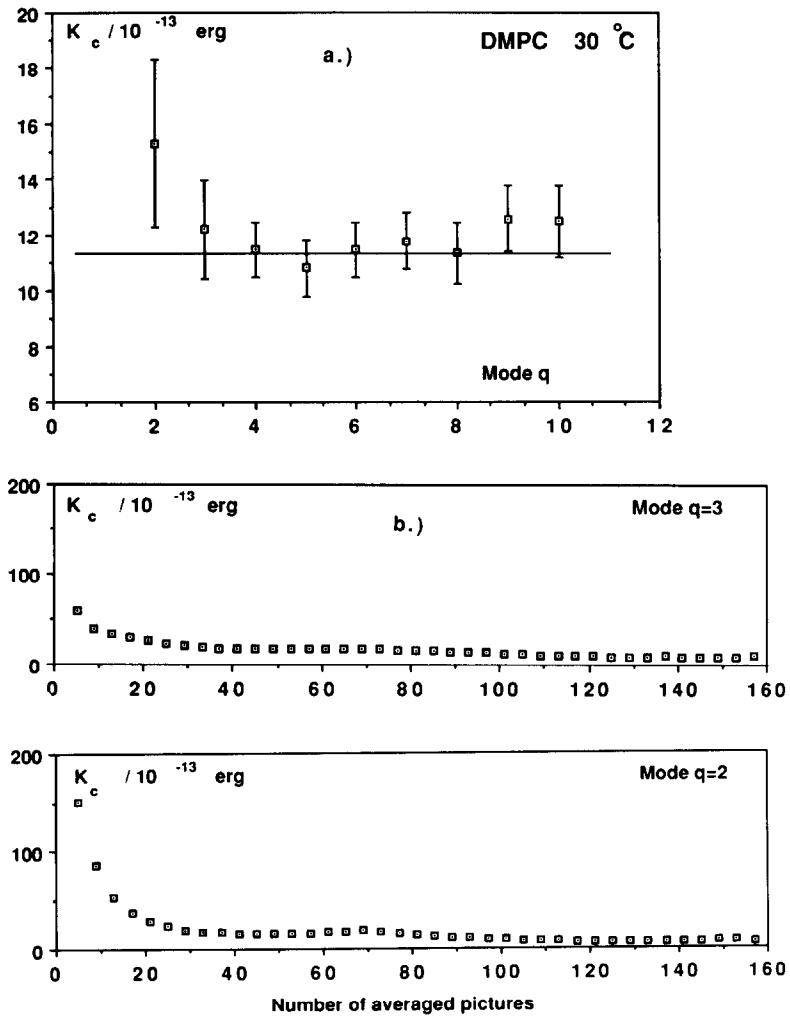

Fig. 3. (a) Bending elastic modulus, K_c, of (most probably) single-walled vesicle of DMPC as function of wave number q characterizing the undulations of the vesicle contour. Vesicle radius $r_0 = 9.91\ \mu$m; temperature $T = 30$°C; 478 images taken at time intervals of 0.2 s were analysed. (b) Value of K_c evaluated for $q = 3$ (top) and $q = 2$ (bottom), respectively, by considering increasing number of images. If the number of averaged images is too small not all excitations of the vesicle are taken into account and the value of K_c becomes too large.

1) In several cases the measured K_c-values clearly form groups. The differences between the average K_c-values of adjacent groups are equal to the lowest values of K_c. Therefore each group of K_c-values corresponds to a vesicle composed of a fixed number of bilayers. The lowest values are attributed to single shell vesicles. This demonstrates the high degree of

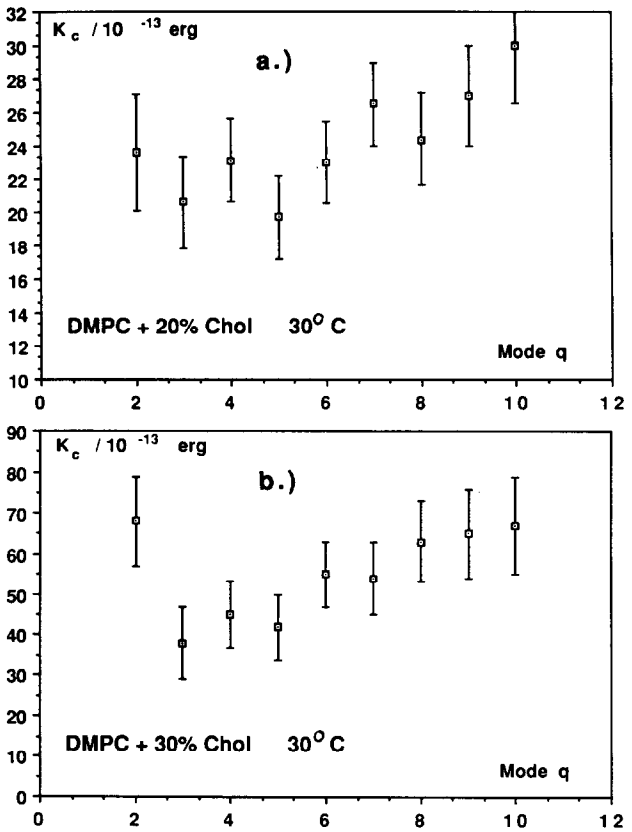

Fig. 4. Bending elastic moduli of single-walled vesicle of DMPC containing (a) 20 mol% and (b) 30 mol% cholesterol, respectively. Measuring temperature: 30°C. Case of fig. 4(a): 176 images taken at time intervals of 0.2 s were analysed; vesicle radius was 9.88 μm. Case of fig. 4(b): 178 images taken at time intervals of 0.25 s were analysed; vesicle radius was 12.19 μm.

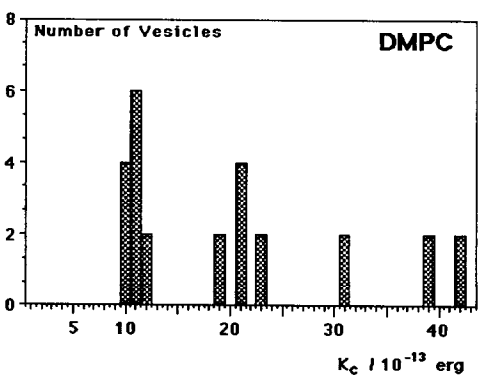

Fig. 5. Summary of average values of K_c measured for DMPC vesicles at 30°C. The ordinate of the histogram gives the numbers of vesicles exhibiting the same bending elastic modulus.

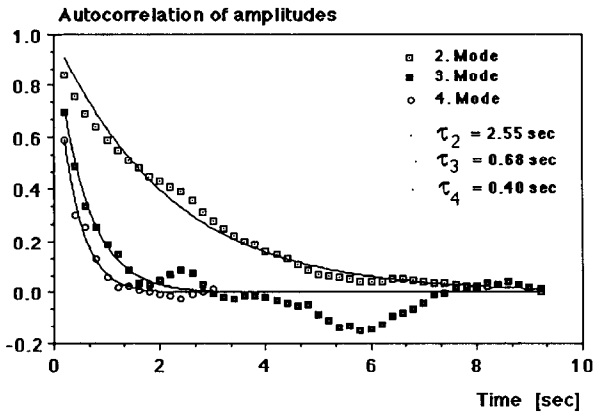

Fig. 6. Plot of autocorrelation function $\langle v_q(t)v_q(0)\rangle$ of amplitudes of contour fluctuations for the three lower order modes. The data points are fitted by single exponential functions using a least-square fitting procedure.

accuracy of the present technique. The average values of the bending moduli of the single shell vesicle are given in table I.

2) Cholesterol leads to a strong increase of the bending stiffness of phospholipid bilayers. This corrobates well with the strong increase of the lateral area compressibility modulus caused by cholesterol [6].

3) Most remarkable is the very low bending modulus of the digalactosyldiglyceride which is about $K_c \approx 3k_BT$. This is partially due to the low area packing density of this lipid. Judged from monolayer studies (at the air–water interface) the area per molecule of this lipid is by about 30% larger (100 Å/molecule) than for DMPC (65 Å^2/molecule).

4) Another remarkable aspect is the rather low bending modulus of the red blood cell membrane. The lipid/protein bilayer of this composite membrane contains about 50% cholesterol and 50% of its total mass is com-

Table I
Summary of average values of bending stiffness of bilayers studied in present work. Most remarkable is the low value of K_c ($\approx 5kT$) for the galactosyldiglyceride and the low value for erythrocytes.

	k_c(erg)
DMPC	$(1.15 \pm 0.15) \times 10^{-12}$
DMPC + 20% cholesterol	$(2.1 \pm 0.25) \times 10^{-12}$
DMPC + 30% cholesterol	$(4.0 \pm 0.8) \times 10^{-12}$
egg–PC	$(1.15 \pm 0.15) \times 10^{-12}$
DMPC + C5-PC (1:1)	$(1.7 \pm 0.2) \times 10^{-12}$
G-DG	$(1.5 - 4) \times 10^{-13}$
Erythrocyte	$(3 - 7) \times 10^{-13}$

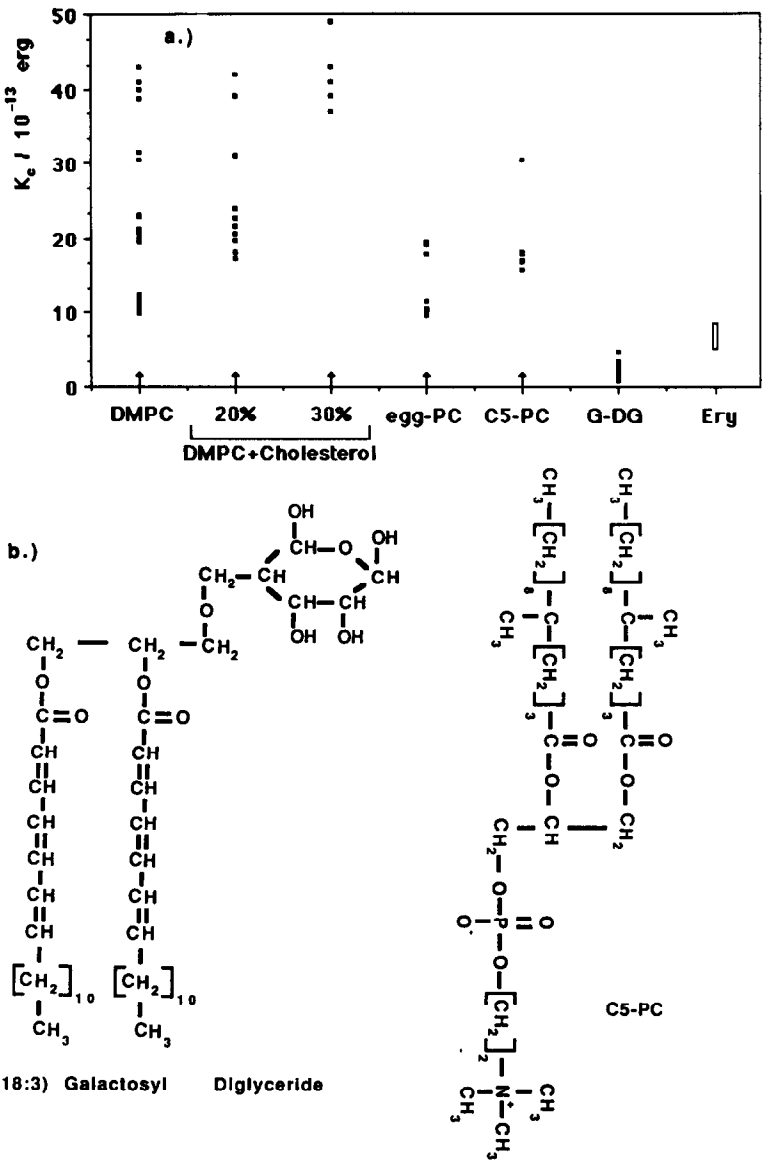

Fig. 7. (a) Summary of bending elastic moduli, K_c, of vesicles of various synthetic and natural lipids and of DMPC–cholesterol mixtures. On the right side the value of red blood cell membrane is shown. The lipid C5-PC is a phosphatidylcholine (PC) with a branched chain. G-DG (=galactosyldiglyceride) is a plant cell lipid with a high content of C = C-double bonds. (b) Structure of lipid C5-PC and G-DG. Each point was obtained by evaluation of one single vesicle. Note that the values for DMPC, DMPC + 20% cholesterol, egg-PC, C5-PC form well-separated groups. The differences between the average values of K_c of adjacent groups are equal to the lowest value of K_c. Thus each group corresponds to vesicles with the same number of bilayers per cell. The lowest average K_c-values are summarized in table I.

posed of integral proteins. One would thus expect a tenfold higher value of K_c. In a forthcoming paper (K. Zeman and E. Sackmann, to be published) we will provide evidence that the bending excitations are determined by the spectrin/actin network coupled to the bilayer.

4.1. Correlation times of membrane excitations

According to eq. (4) the dynamics of each spherical harmonic mode is determined by an exponential autocorrelation function. Since the mean square amplitude of each contour excitation of wave vector q is the sum over the mean square amplitudes $|a_{l,m}^2|$, the autocorrelation function $\langle v_q(t)v_q(0)\rangle$ is also a sum over exponentials. However, it can be well approximated by a simple exponential with the decay constant (reciprocal correlation time) $\omega_q = \omega_l$ for the following reasons. Firstly the lowest order term of each sum is $q = 1$ (cf. eq. (8)). Secondly, the correlation time ω_l increases approximately with the third power of l and the amplitudes $a_{l,m}^2$ decrease with the fourth power of l. The autocorrelation functions, $A_q(\tau)$, of the three lowest order modes ($q = 2$, 3 and 4) of the contour fluctuations were directly determined from the amplitudes $v_q(t)$ according to

$$A_q(\tau) = \frac{1}{S}\,\frac{1}{N-t}\sum_n v_q(t_n)v_q(t_n+\tau)\,,$$
$$S = \frac{1}{N} = \sum n\,|v_q(t_n)|^2\,. \tag{14}$$

The autocorrelation functions thus determined are plotted in fig. 6 for the three lowest order modes ($q = 2$, 3, 4). The experimental data can be well fitted by a single exponential function. The oscillations of the experimental plots of $A_q(t)$ are due to experimental errors and/or slow Brownian motion of the whole vesicle during the measurement. The correlation times of the three lowest order modes are summarized in table II and compared with values (denoted as theoretical in table II) calculated from eq. (5) with the measured values of K_c

Table II
Comparison of experimental with theoretical relaxation times $\tau_l = \omega_{l,m}^{-1}$ for modes $q = 2$ to $q = 4$ as calculated for $\gamma = 0$ and $\gamma = -2.3$. Vesicle radius $r_0 = 9.91\ \mu$m, $K_c = 1.1 \times 10^{-12}$ erg and water viscosity $\eta = 1.002$ mP.

	Relaxation time (s)		
	τ_2	τ_3	τ_4
Theoretical: $\gamma = 0$	3.34	0.99	0.43
Theoretical: $\gamma = -2.3$	2.45	0.83	0.38
Experimental	2.55	0.68	0.40

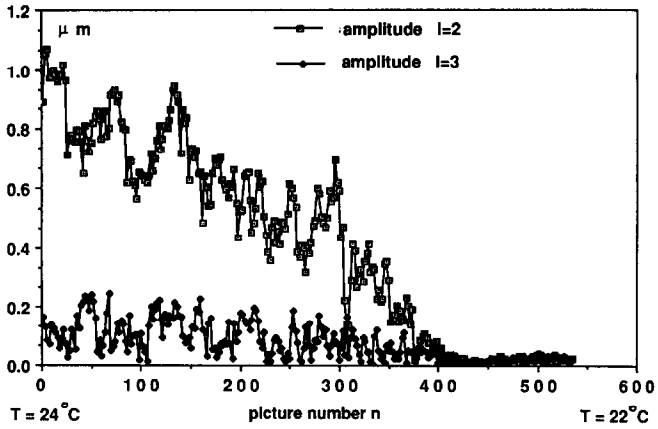

Fig. 8. Plot of mean square amplitudes of 2nd and 3rd order modes of DMPC bilayer vesicle as a function of temperature upon approaching the fluid-to-solid phase transition. The (chain) melting ($P_{\beta'}$–L_α transition) temperature of DMPC is $T_m = 23.8$°C.

and the average vesicle radius r_0. For $\gamma = 0$ one observes a systematic discrepancy between calculated and experimental values. Good agreement is, however, observed for a value of $\tilde{\gamma} = -2.3$. This value has indeed been obtained by fitting the apparent value of K_c for the lowest order mode ($q = 2$) to the values obtained for $q \geq 3$. We thus conclude that both the dynamic and the equilibrium model of the vesicle fluctuation [15] agree well with experimental data.

4.2. *Freezing of undulations at the L_α–$P_{\beta'}$ phase transition*

Fig. 8 shows the temperature dependence of the mean square amplitudes of the second and third order modes in the neighbourhood of the fluid-to-solid (L_α–$P_{\beta'}$) transition of a DMPC bilayer vesicle. Clearly, the higher order modes freeze in at higher temperature than the second order excitation. This is largely a consequence of the reduction of the vesicle area and the corresponding increase of the influence of the surface tension (γ). The gradual freezing in of the long-wavelength excitations well above the transition temperature ($T_m = 23.8$°C) may be the origin of the precritical behaviour of the phase transition.

5. General discussion

5.1. *Breakdown of bending mode concept at short wavelengths*

The present Fourier analysis of the shape fluctuations of vesicles allows one to determine the membrane bending elastic modulus to an accuracy of 10%. In

particular shells composed of different numbers of bilayers may well be distinguished. The detailed study of DMPC showed that the quasi-spherical model can well describe the static and the dynamic aspects of the membrane excitations. The bending mode concept certainly breaks down at wavelengths comparable to the bilayer thickness ($\approx$10 nm) where the undulations are expected to be associated with lateral tension and with shear deformations in the direction of the membrane normal [11]. However, the present measurements at cholesterol containing lipid bilayers show that in this particular case the bending mode concept breaks down even in the optical wavelengths regime. There are two reasons for this breakdown: (1) the shear associated with the mutual shift of the opposing monolayers and (2) the lateral pressure arising in both monolayers if the lipid flow is too slow to accommodate the local density fluctuations. We favour the latter effect as a possible explanation for two reasons: firstly, the lateral compressibility modulus is strongly increased by cholesterol (by a factor of four at 30 mol% cholesterol) and secondly, the lateral mobility is substantially reduced (by about a factor of two at 30% cholesterol).

The effect of the shear associated with the monolayer–monolayer slip depends on their coupling strength. Recent lateral diffusion measurements on supported bilayers [14] provide evidence for such strong coupling. The impeded monolayer slip certainly comes into play in the 100 nm regime as shows the following consideration: According to eq. (5) and table II, the relaxation time of the undulations of order l is $\tau_{rel} = 2.7 \times 1^{-3}$ s whereas the undulations wavelengths scale (with l) as $=2\pi r_0/l$. On the other hand, the reciprocal jump frequency of the lipid lateral Brownian motion is $\approx 10^7\ s^{-1}$. Thus the monolayer–monolayer shearing is expected to become essential for $l \approx 1500$ or for undulation wavelengths of $\leqslant$50 nm.

5.2. *Bending elasticity and vesicle shape fluctuations*

Fig. 9 shows a series of transient shapes of vesicles with decreasing bending elastic moduli. Fig. 9(a) shows the case of DMPC at a temperature slightly above and below the L_α-to-$P_{\beta'}$ transition. In the latter case the shape depends on the excess area. If it is small the shape is quasi-spherical while at large excess areas the vesicles assume a pronounced polygonal shape. Both cases are shown. Fig. 9(b) shows the case of galactosyldiglyceride which forms quasi-spherical vesicles if the excess area is small tubules if it is large. The thermal excitations are clearly much more pronounced than for DMPC owing to the nearly fivefold lower K_c-value.

A particular interesting example is shown in fig. 9(c). A small amount (5 mol%) of a bipolar amphiphile (called bola-lipid) (shown below) is added to DMPC.

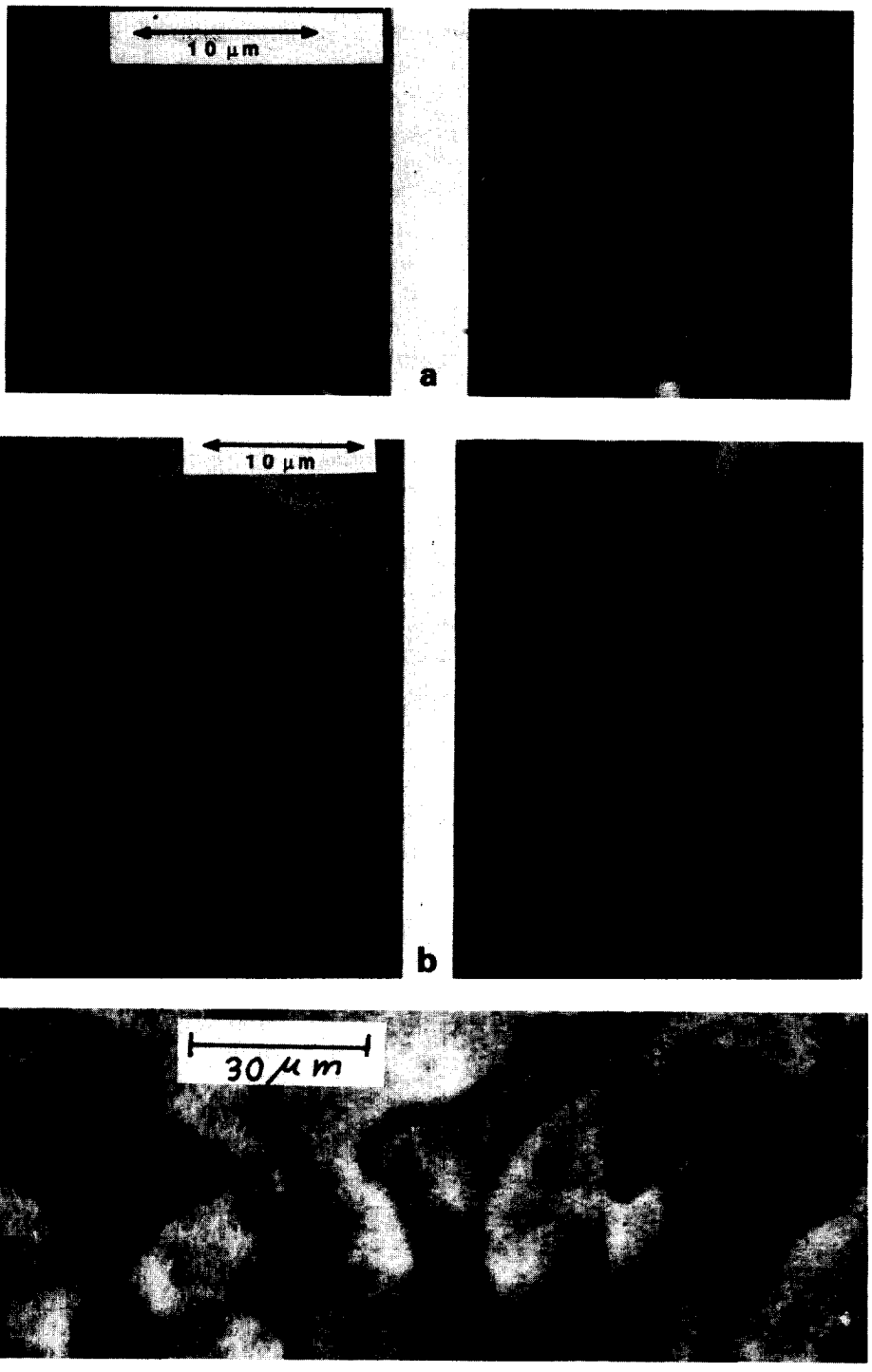

Fig. 9 (see overleaf).

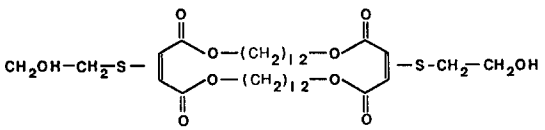

BOLA - Lipid

This small amount of solute causes extremely strong fluctuations which are so fast that the contour becomes completely smeared out and a Fourier analysis is no longer possible. A rough estimate shows that the mean square amplitudes become of the order of 1 μm at wavelengths of about 5 μm for a vesicle of $r_0 \approx 10$ μm which corresponds to $l \approx 5$. K_c is thus of the order of $(0.1\text{–}1)kT$ (for $\gamma = 0$). The strong fingering of the vesicle shows that it is a good approximation of a random surface. The extension of the fingering is most probably limited by the surface tension γ. The vesicles are very unstable and gradually decay by splitting-off of small vesicles which remove the highly disturbing bipolar lipid. The origin of the strong reduction in K_c is not known yet and it may well be associated with transient precipitation of the bipolar lipid. Since the length of its hydrophobic chain equals half the bilayer thickness one expects that the bola-lipid enforces phospholipid chain interdigitation at least in its neighbourhood as indicated in fig. 10.

The effect of the bola-lipid is one example of a manifold of new phenomena arising in membranes of lipid mixtures. In these cases the structure and dynamics of vesicles is also determined by the coupling between curvature and lateral phase separation. This leads to metastable domain structures of membranes (Gebhardt et al. [8], Petrov et al. [18] which can be described in terms

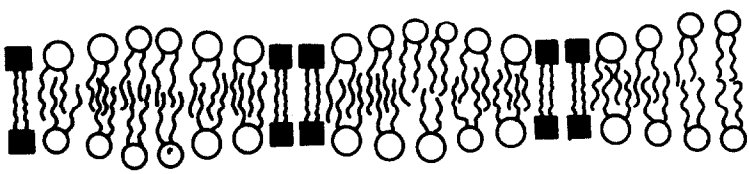

Fig. 10. Possible structure of DMPC containing 5 mol% of short bipolar lipid (called bola-lipid). In order to accomodate this lipid (the hydrophobic center of which is half as long as the bilayer thickness) the DMPC is expected to be interdigitated at least in the neighbourhood of (possible precipitated) bola-lipid molecules.

Fig. 9. Transient shapes of vesicles with the bending modulus decreasing from a to c. (a) Vesicle of DMPC. Left: (24°C) slightly above chain melting transition T_m; right: (22°C) slightly below T_m; $T_m = 23.8$°C, $K_c = 1.1 \times 10^{-12}$ erg. (b) Quasi-spherical (left) and tube-like (right) vesicles of galactosyldiglyceride at 20°C. Vesicle is composed of two bilayers $K_c \approx 2 \times 10^{-13}$ erg. (c) Vesicles of DMPC containing 5 mol% of a bipolar lipid (the so-called bola-lipid) shown in the text. Images taken at $T = 24$°C. Judged from the amplitudes the bending stiffness is $K_c \approx kT$.

Fig. 11. Metastable shape of vesicle of DMPC containing 30 mol% cholesterol at 27°C. The vesicle fluctuates slightly about the cross-like form.

of a Landau–Ginzburg equation (Wonneberger [22], Leibler and Andelman [13]). An example of the peculiar vesicle shapes observed in these cases is shown in fig. 11.

Acknowledgements

This manuscript was partially written during a visit at the University of British Colombia in Vancouver and one of the authors (E.S.) is most grateful to E.A. Evans for his hospitality and for many enlightening discussions. We also grately profited from helpful discussion with W. Helfrich, S. Leibler, R. Lipowski and St. Millner. Last not least we would like to thank H. Engelhardt who pioneered the present dynamic image processing technique. The work was financially supported by the Deutsche Forschungsgemeinschaft (Project Sa 246/16-2 and SFB 266) and by the Fonds der Chemischen Industrie.

References

[1] G. Beblik, R.M. Servuss and W. Helfrich, J. Physique 46 (1985) 1773.

[2] I. Bivas, P. Hanusse, P. Bothorel, J.L. Lallane and O. Aguerre-Chariol, J. Physique 48 (1987) 855.
[3] F. Brochard and J.F. Lennon J. Physique 36 (1975) 1035.
[4] H.P. Duwe, P. Eggl and E. Sackmann, Die Angewandte Makromolekulare Chemie 166/167 (1989) 1.
[5] H. Engelhardt, H.P. Duwe and E. Sackmann, J. Phys. Lett. (Paris) 46 (1985) 395.
[6] E.A. Evans and D. Needham, Faraday Discuss. Chem. Soc. 81 (1986) 267.
[7] H.J. Galla, W. Hartmann, U. Theilen and E. Sackmann, J. Member. Biol. 48 (1979) 215.
[8] G. Gebhardt, H.Gruber and E. Sackmann, Z. Naturforsch. (c) 32 (1977) 581.
[9] W. Helfrich, Z. Naturforsch. (c) 28 (1973) 693.
[10] W. Helfrich, J. Physique 47 (1986) 321.
[11] M.M. Kozlov and U.S. Markin, J. Chem. Soc. Faraday Trans. 2 (1989) 85.
[12] L.D. Landau and E.M. Lifschitz, Theory of Elasticity (Pergamon, New York, (1970).
[13] S. Leibler and D. Andelman, J. Physique 48 (1987) 2013.
[14] R. Merkel, E.A. Evans and E. Sackmann, J. Physique 50 (1989) 1535.
[15] S.T. Millner and S.A. Safran, Phys. Rev. A 36 (1987) 4371.
[16] K. Niederdrenk, Die endliche Fourier- und Walsh Transformation mit einer Einführung in die Bildverarbeitung, 2nd ed. (Vieweg, Braunschweig, 1984).
[17] M.A. Peterson, Mol. Cryst. Liq. Cryst. 127 (1985) 257.
[18] A.G. Petrov, M.D. Mitov and A.I. Derzhanski, in: Advances of Liquid Crystal Research and Application, L. Bata, ed. (Pergamon, Oxford, 1980).
[19] W. Pfeiffer, Th. Henkel, E. Sackmann, W. Knoll and D. Richter, Europhys. Lett. 8 (1989) 201.
[20] E. Sackmann, H.P. Duwe and W. Pfeiffer, Physica Scripta T 25 (1988) 107.
[21] M.B. Schneider, J.T. Jenkins and W.W. Webb, J. Phys. (Paris) 45 (1984) 1457.
[22] W. Wonneberger, Z. Phys. B-Condensed Matter 46 (1982) 73.
[23] A. Zilker, H. Engelhardt and E. Sackmann, J. Physique 48 (1987) 2139.